The sintered high purity polycrystalline alumina specimens fired in Cr_2O_3 at 1675° C for 3 h showed an increase in average flexural strength at elevated temperatures when compared to control specimens given the same thermal treatment. However, they showed the same proportional reduction in strength with temperature as the untreated materials. The sharp decrease in strength at high temperatures, which may be due to grain-boundary sliding, was almost independent of thermal and chemical treatment.

Acknowledgement

This work was sponsored by the Engineering Research Institute at Iowa State University through funds provided by the Aerospace Research Laboratories, Office of Aerospace Research USAF, under contract No. F33615-68-C-1034.

References

1. K. M. MERZ, W. R. BROWN and H. P. KIRCHNER, *J. Amer. Ceram. Soc.* **45** (1962).
2. H. P. KIRCHNER and R. M. GRUVER, *ibid* **49** (1966) 330.
3. H. P. KIRCHNER, R. M. GRUVER and R. E. WALKER, *ibid* **51** (1968) 251.
4. *Idem, J. Appl. Phys.* **40** (1969) 3445.
5. J. T. FRASIER, J. T. JONES, K. S. RAGHVAN, T. D. McGEE and H. BELL, *Amer. Ceram. Soc. Bull.* **50** (1971) 541.
6. R. M. SPRIGGS, "Mechanical and Thermal Properties of Ceramics", edited by J. B. Wachtman, Jun., Nat. Bur. Stand. USA, Spec. Publ. No. 303 (1969) p. 189.

Received 28 October 1975
and accepted 26 July 1976

S. M. OH
Department of Metallurgy & Materials Science, Case Western Reserve University, Cleveland, Ohio, USA
J. T. JONES
The Pfaltzgraff Co., York, Pennsylvania, USA

A TEM investigation of hydrogen-induced deformation twinning and associated martensitic phases in 304-type stainless steel

Twinning is well known to be one of the basic processes available for plastic deformation in metals [1]. Previous studies [2–5] have shown twinning to be a common deformation mechanism for mechanically strained fcc single-crystal thin films. The purpose of this article is to report the results of a TEM analysis of twins and associated martensitic phases produced by cathodic hydrogen charging of polycrystalline austenitic stainless steel thin foils, in the absence of any externally applied stress. The microstructural characteristics of the hydrogen- and strain-induced deformation twins will be compared.

The specimens used in the strain-induced deformation twin studies [2–5] were produced by vacuum evaporation of pure metals onto (0 0 1) cleaved alkali halide substrates to give (0 0 1) oriented thin films. Mechanical straining of the specimens, at relatively low strain-rates and along specific crystal directions in the (0 0 1) thin-film plane, produced deformation twins on the usual $\{1\,1\,1\}\cdot\langle 1\,\bar{1}\,0\rangle$ fcc twin systems. The deformation twinning was found to occur in very localized regions within the thin foils. With increasing deformation, plastic strain occurred preferentially within the twinned regions, causing the regions to increase in size and local thinning to occur. This process eventually resulted in the formation of cracks within the twinned regions.

Disc specimens of a fully recrystallized 18-8 type stainless steel were prepared using a dish technique [6] to produce a thinned centre region suitable for TEM and supported by a relatively thick outside rim. After a TEM examination to ensure that no deformation structure has been induced during preparation, the specimens were cathodically hydrogen charged. Using a 1 N sulphuric acid solution at room temperature which contained $0.2\,g\,l^{-1}$ arsenic trioxide to inhibit hydrogen recombination at the specimen surface, cathodic charging times varied from a few seconds to a few minutes with a current density of $0.2\,A\,cm^{-2}$. Chemical analysis of the material used in this study is given in Table I.

Fig. 1a shows a hydrogen-induced deformation

TABLE I Chemical analysis (wt %)

Fe	Cr	Ni	C	Mn	Si	Cu	Mo	Co	P	S
Bal.	18.34	0.66	0.074	1.30	0.50	0.14	0.13	0.10	0.014	0.009

twinned (HIDT) region which lies along X–X′ and which crosses through a grain containing two annealing twins. In region A of Fig. 1a, the specimen foil is fractured with the crack propagating along the HIDT region. Trace analysis revealed that the zig-zag path of the HIDT region allowed

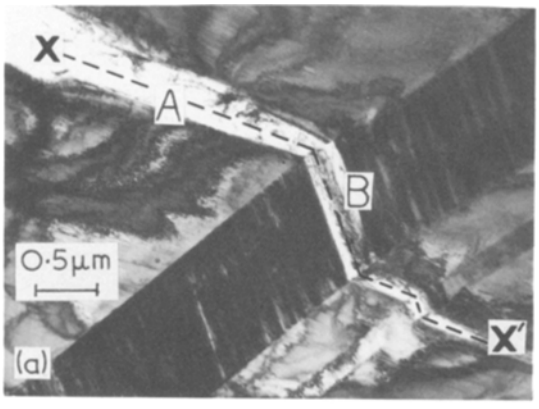

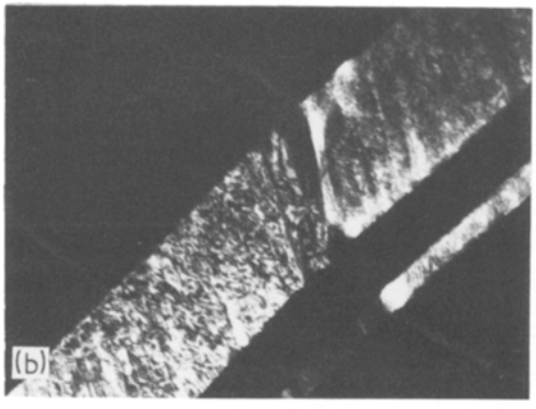

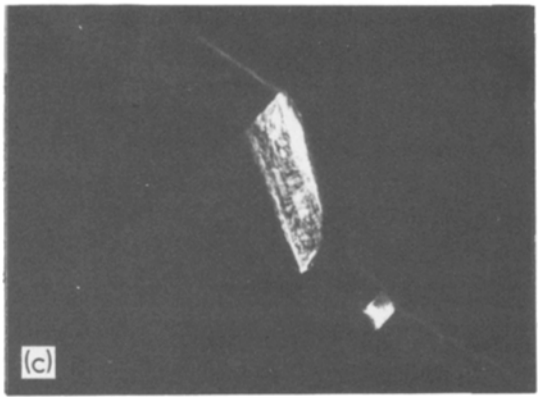

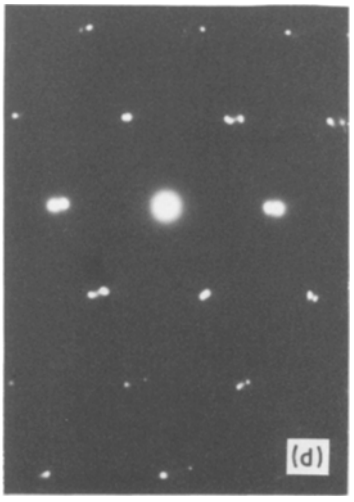

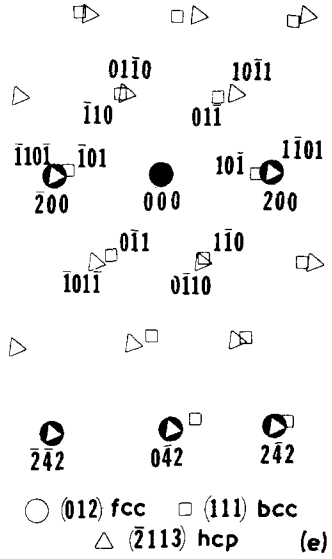

Figure 1 (a) TEM bright-field micrograph of a hydrogen-induced deformation twinned region. (b) TEM dark-field micrograph of ϵ_M (h c p) martensite. (c) TEM dark-field micrograph of α_M (b c c) martensite. (d) Electron diffraction pattern from region B of (a). (e) Indexed version of (d).

the region to follow $\{1\,1\,1\}_\gamma$ planes in both the matrix and the annealing twins. The preference of HIDT regions to follow particular planes, by abruptly changing propagation directions upon passing from one grain into another, was a common characteristic of all regions studied. Fig. 1d and e show experimental and indexed versions, respectively, of an electron diffraction pattern from area B in Fig. 1a. Diffraction analysis of area B revealed two additional phases, ϵ_M (h c p) and α_M (b c c) martensites, associated with the HIDT region contained within the annealing twin. Using electron diffraction and stereographic projection techniques, the f c c/ϵ_M and f c c/α_M orientation relationships were determined to be: $(1\,1\,1)_\gamma \parallel (0\,0\,0\,1)\epsilon_M$, $[0\,1\,\bar{1}]_\gamma \parallel [\bar{1}\,2\,\bar{1}\,0]\ \epsilon_M$ and $(1\,1\,1)_\gamma \parallel (1\,1\,0)\alpha_M$, $[\bar{2}\,1\,1]_\gamma \parallel [\bar{1}\,1\,0]\,\alpha_M$. These orientation relationships for hydrogen-induced ϵ_M and α_M agree with those reported for strain-induced ϵ_M and α_M [7, 8]. Fig. 1b and c show dark-field

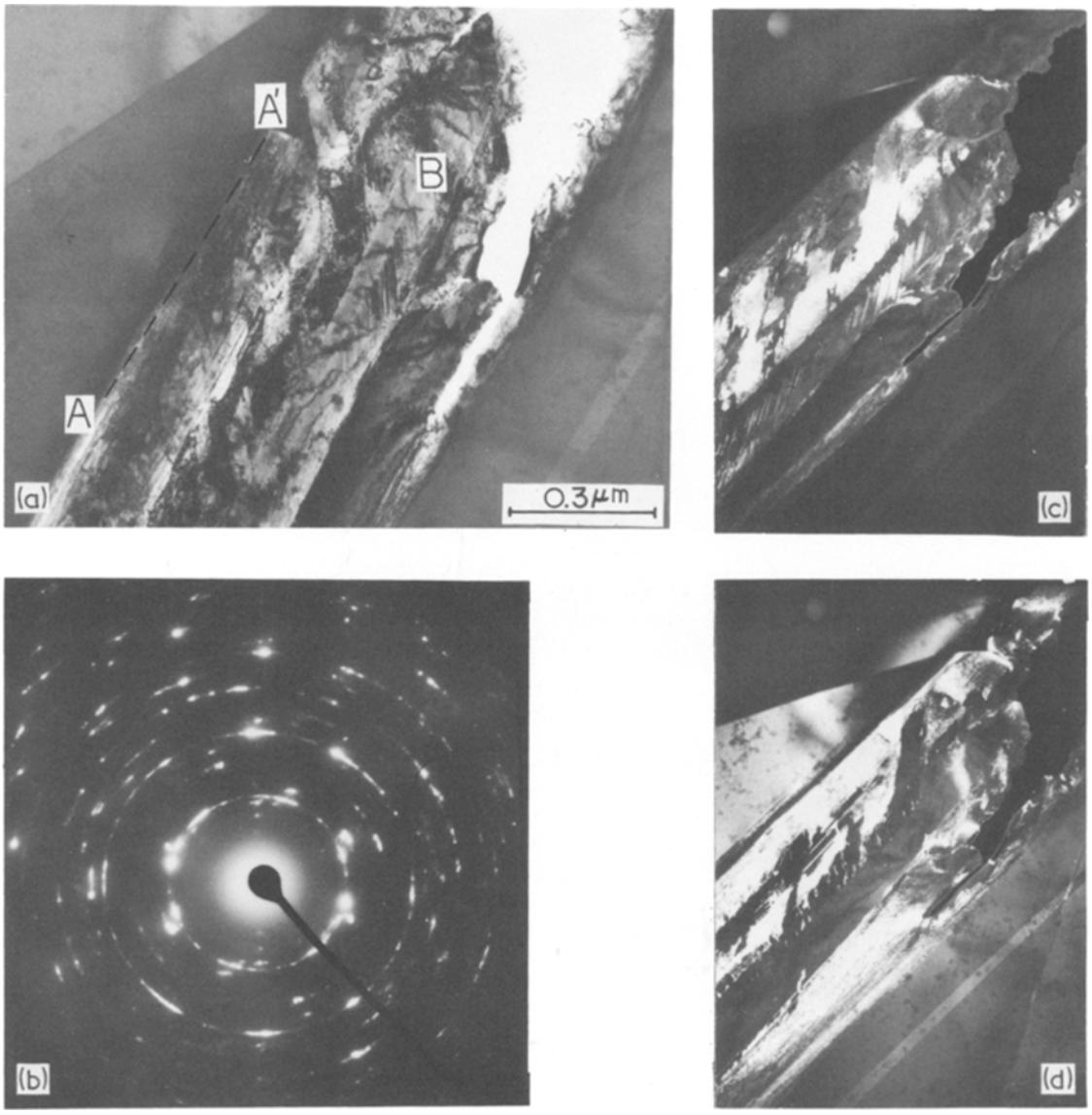

Figure 2 (a) TEM bright-field micrograph of a hydrogen-induced deformation twinned region. (b) Electron diffraction pattern from region B of (a). (c) TEM dark-field micrograph of ϵ_M martensite. (d) TEM dark-field micrograph of hydrogen-induced deformation twins.

micrographs of the ϵ_M and α_M phases respectively.

Fig. 2a is a bright-field micrograph of a HIDT region which formed along a $\{1\,1\,1\}_\gamma$ plane parallel to the annealing twin boundary A–A′. The bands in the HIDT region and parallel to A–A′ are the deformation twins and the fine, closely spaced line structures crossing the banded regions are ϵ_M. As was common for well developed HIDT regions, a crack was observed along the general direction of the deformation twins. Fig. 2b is an electron diffraction pattern from area B of Fig. 2a. From interplanar spacings [9] obtained from the radii of circles drawn through the various groups of diffraction spots in Fig. 2b, both deformation twins and ϵ_M are present in the HIDT region. The ϵ_M visible in the dark-field micrograph of Fig. 2c again consists of a fine, closely spaced line structure. Fig. 2d is a dark-field micrograph which shows some of the deformation twinned regions.

Since the microstructure and the deformation-fracture process of the HIDT regions are similar to those of the strain-induced deformation twinned regions [2–5] and since HIDT was not found in bulk TEM specimens thinned finally after cathodic charging, HIDT appears to be a thin-foil phenomena. However, in addition to the unique presence of the associated hydrogen-induced martensitic phases, the HIDT regions were usually composed of several individual deformation twins ranging from 250 to 500 Å in width. This contrasts with the strain-induced deformation twin regions which were apparently composed of a single wide twin.

References

1. S. MAHAGAN and D. F. WILLIAMS, *Int. Met. Rev.* 18 (1973) 43.
2. J. W. MATTHEWS, *Acta. Met.* 18 (1970) 175.
3. R. E. WINTER and J. E. FIELD, *Phil. Mag.* 29 (1974) 395.
4. S. MARUYAMA and H. KIHO, "Electron Microscopy: Sixth International Congress for Electron Microscopy", Vol. 1 (Maruzen, Kyoto, 1966) p. 311.
5. A. CATLIN, W. P. WALKER, K. R. LAWLESS, *Acta. Met.* 8 (1960) 734.
6. C. K. H. DUBOSE and J. O. STIEGLER, *Rev. Sci. Instrum.* 38 (1967) 694.
7. R. LAGNEBORG, *Acta. Met.* 12 (1964) 823.
8. H. FUJITA, and S. UEDA, *ibid.* 20 (1972) 759.
9. M. L. HOLZWORTH and M. R. LOUTHAM, JUN., *Corrosion* 24 (1968) 110.

Received 21 June
and accepted 19 July 1976

J. M. RIGSBEE*
Department of Metallurgical Engineering, Michigan Technological University, Houghton, Michigan, USA
R. B. BENSON, JUN.
Department of Materials Engineering, North Carolina State University, Rayleigh, North Carolina, USA

*Present address: Republic Steel Research Center, 6801 Brecksville Road, Cleveland, Ohio, USA

Growth of oxide in situ composites: the systems lithium ferrite–lithium niobate, lithium ferrite–lithium tantalate, and nickel ferrite–barium titanate

The general utility of capillary shaping techniques were recently evaluated [1–4] for growing ceramic *in situ* composites [4] to be used in non-structural applications. During these studies we identified three new oxide-phase systems for which directional freezing produces well-aligned composite microstructures: lithium ferrite–lithium niobate, lithium ferrite–lithium tantalate, and nickel ferrite–barium titanate. The melting relations for these systems and the morphological characteristics of the directionally frozen composites are reported here.

Often the phase relations for attractive ternary and higher order oxide systems are too fragmentary or imprecisely known to select melt compositions for composite growth. Therefore, we melted and cast representative compositions from candidate systems and searched the specimen microstructures for morphologically uncomplicated two-phase aggregates. Three systems, $Li_{0.5}Fe_{2.5}O_4$–$LiNbO_3$, $Li_{0.5}Fe_{2.5}O_4$–$LiTaO_3$, and $NiFe_2O_4$–$BaTiO_3$, yielded promising microstructures; for these systems partial phase diagrams were constructed from cooling curves, X-ray diffraction and microstructural data.

The cooling curves were developed by monitoring the output of a Pt/Pt–6% Rh thermocouple immersed in 40 g charges of each oxide melt. The temperature was cycled several times through the